

Supporting Information

Printed Thin Diblock Copolymer Films with Dense Magnetic Nanostructure

Senlin Xia[†], Lin Song^{†,§}, Wei Chen[†], Volker Körstgens[†], Matthias Opel[‡], Matthias Schwartzkopf[§], Stephan V. Roth^{§,¶}, Peter Müller-Buschbaum^{, †, §}*

[†]Technische Universität München, Physik-Department, Lehrstuhl für Funktionelle Materialien, James-Frank-Straße 1, D-85748 Garching, Germany

[§]Institute of Flexible Electronics, Northwestern Polytechnical University, West Youyi Road 127, 710072, Xi'an, Shanxi, China

[‡]Walther-Meissner-Institut, Bayerische Akademie der Wissenschaften, Walther-Meissner-Str. 8, D-85748 Garching, Germany

[§]Deutsches Elektronen-Synchrotron DESY, Notkestrasse 85, D-22603 Hamburg, Germany

[¶]KTH Royal Institute of Technology, Department of Fibre and Polymer Technology, Teknikringen 56-58, SE-100 44 Stockholm, Sweden

[§]Heinz Maier-Leibnitz Zentrum (MLZ), Technische Universität München, Lichtenbergstr. 1, D-85748 Garching, Germany

KEYWORDS: thin, diblock copolymer, magnetic nanoparticles, GISAXS, dense magnetic structure, superparamagnetic behavior

Corresponding Author

* Email: muellerb@ph.tum.de

Characterization Techniques

Optical Microscopy (OM)

The macroscopic surface structure was probed with an Axiolab A microscope (Carl Zeiss), which enabled the use of five different magnifications. Images were taken with a PixeLink USB Capture BE 2.6 charge coupled device (CCD) camera. Different magnifications were tested for all samples.

Profilometry:

The thickness of the printed thin films was examined with a profilometer (Dektak XT Surface Profiler, Bruker). The profilometer was set with a stylus force of 9.8 μN and a scan speed of 1 $\mu\text{m/s}$ for the measurements. The films were first scratched with a plastic knife to expose the substrate, then measured at 10 different spots. Afterwards, an average film thickness was calculated.

Atomic Force Microscopy (AFM)

AFM measurements were carried out thorough a MFP-3D AFM (Asylum Research) using tapping mode under ambient conditions. The applied tip had a curvature radius of 7 nm and was positioned onto cantilevers (OMCL-AC240TS-R3, Asylum Research) with a spring constant as 2 N/m and a resonance frequency of 70 kHz. The software Gwyddion 2.42 was used for data process and analysis.

Scanning Electron Microscopy (SEM)

SEM was probed by An NVision40 FESEM (Carl Zeiss AG). In order to obtain a better contrast in the SEM images, all films showed in the main text were treated with oxygen plasma for 10 s before the SEM measurements. The plasma etcher Diener NANO functioned at a power density of 8.3 W/dm^3 (200 W in total). For further morphology demonstration, the film showed in the supporting information was etched for 30 s. During the measurement, the accelerating voltage was 1.5 kV with working distances of 1.7 mm. In order to check the homogeneity of films, several random spots across each sample were probed.

Grazing Incidence Small-Angle X-ray Scattering (GISAXS)

X-ray scattering measurements were carried out at the Micro- and Nano focus X-ray Scattering (MiNaXS) beamline P03 located inside the PETRA III storage ring (DESY, Hamburg, Germany).¹⁻² Photon energy of 13.2 keV with corresponding wavelength ($\lambda = 0.094 \text{ nm}$) was applied. The incidence angle impinging onto the films was chosen as 0.35° , which was well above the critical angles (total reflection angles) of all involved materials in the magnetic thin films. Thus, the entire films were probed by the X-ray beam, and averaged structural information of the whole depth of the films was obtained. During the GISAXS measurements, a 2D detector with pixel size $172 \times 172 \text{ }\mu\text{m}^2$ (Pilatus 1M Dectris Ltd., Switzerland) was placed at a sample-to-detector distance of 4377 mm to collect the scattering signals. To protect the detector from oversaturation, two point-like beamstops were placed in front of the detector at the positions of specular peak and direct beam. To avoid beam damage, all films were measured on several different spots respecting the maximum exposure time before radiation damage sets-in. Lateral structural information was achieved from the horizontal line cuts (q_y direction, parallel to the sample surface) made on the 2D GISAXS data. For detailed

analysis, all q_y profiles were fitted with a model assuming a Lorentzian distribution of length scales.

Magnetic Property Measurements (MPM)

A superconducting quantum interference device (SQUID) magnetometer (MPMS XL-7, Quantum Design, San Diego, CA) was employed for carrying out magnetization measurements at different fields and temperatures. The data were taken in DC (direct current) or RSO (reciprocating sample option) mode in external magnetic fields ranging from -700 to 700 mT applied in the film plane. All samples were studied at six different temperatures: 2 , 5 , 20 , 50 , 100 , and 200 K. All relevant data were obtained in the reciprocating sample option (RSO) mode at each fixed temperature. The error in temperature can be considered below 0.1 K. The error in magnetic moment depends on the overall signal (i.e. the emu range of the instrument) and on the applied magnetic field. Based on the documentation of Quantum Design, the error is 1×10^{-8} emu = 1×10^{-11} Am² or 0.1% for a field range below 2500 Oe = 250 mT.

¹H-NMR Spectrum of PS-*b*-PMMA

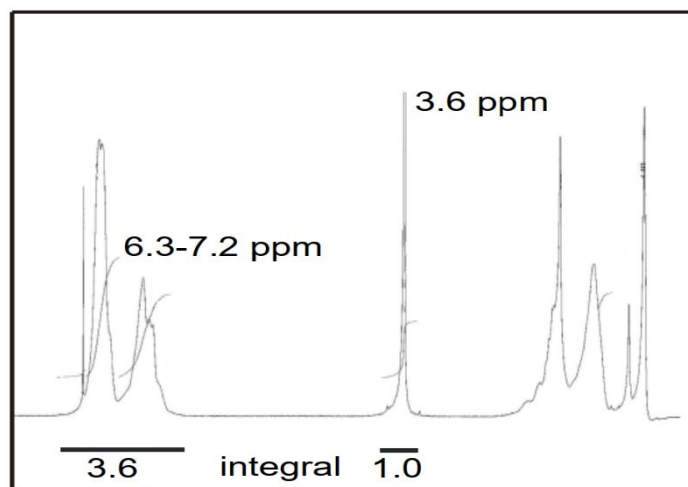


Figure S1. ¹H-NMR Spectrum of PS-*b*-PMMA. Data is provided by the polymer supplier Polymer Source, Inc.

The final block copolymer composition was calculated from ¹H-NMR spectroscopy (Figure S1) by comparing the peak area of the poly(methyl methacrylate) protons (eg. –OCH₃ at 3.6 ppm) with the aromatic protons of polystyrene at 6.3-7.2 ppm.

Demonstration of the cylindrical morphology

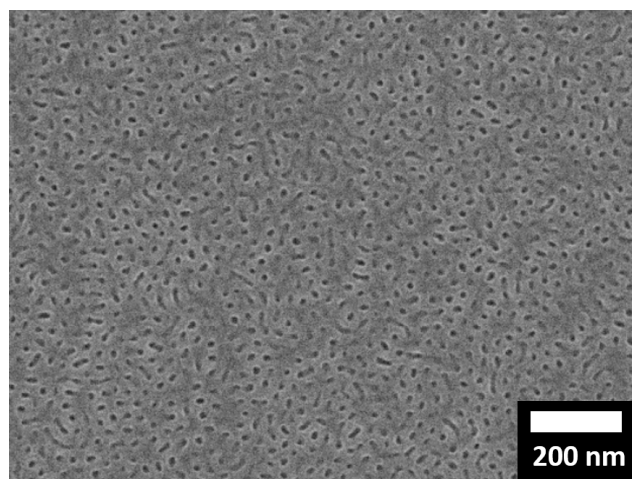


Figure S2. SEM of the pure PS-*b*-PMMA film with the thickness of 50 nm. The film was strong etched for 30 s before the SEM measurement.

Localization of MNP inside PS domains

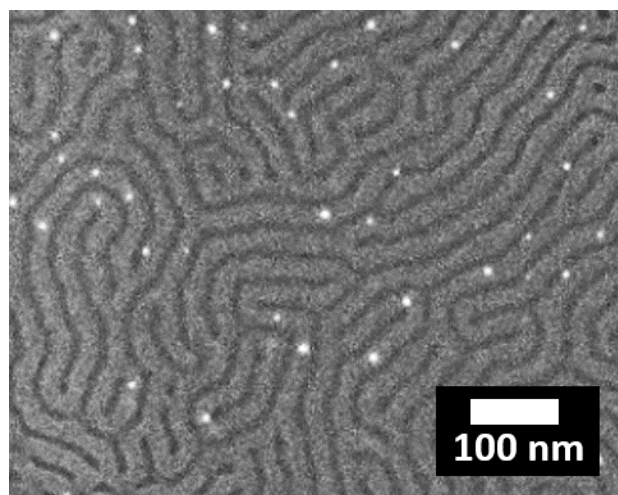


Figure S3. SEM of the PS-*b*-PMMA film with 3 wt % MNPs at higher magnification. The preference of NPs to the brighter PS domains is evidenced.

Root mean square roughness (R_{rms}) of films

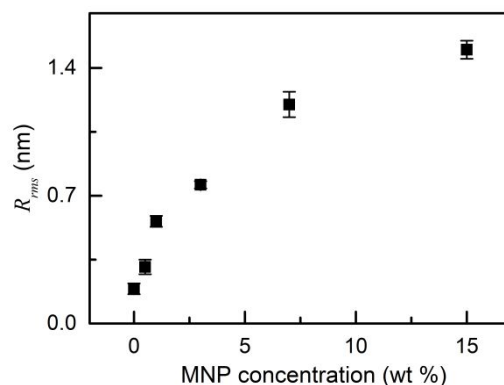


Figure S4. Root mean square roughness (R_{rms}) as a function of MNP concentration. The R_{rms} is obtained using the software Gwyddion. Five random areas are chosen for roughness calculation in each image and averaged.

Intensity increment of the first and second order peak in the hybrid DBC structure upon MNP loading

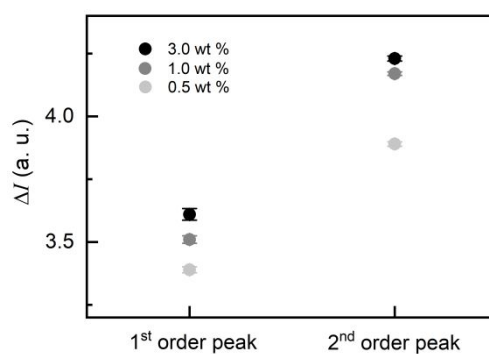


Figure S5. Intensity increment ΔI of the structure peaks (the first and second order peaks) at different MNP concentrations. ΔI is calculated by $I_{\text{hybrid-}i} / I_{\text{pure-}i}$, where $I_{\text{hybrid-}i}$ and $I_{\text{pure-}i}$ are the intensity of the peak in the hybrid and pure film, respectively. $i = 1, 2$ shows the peak order.

Values of full width at half maximum as a function of MNP concentration

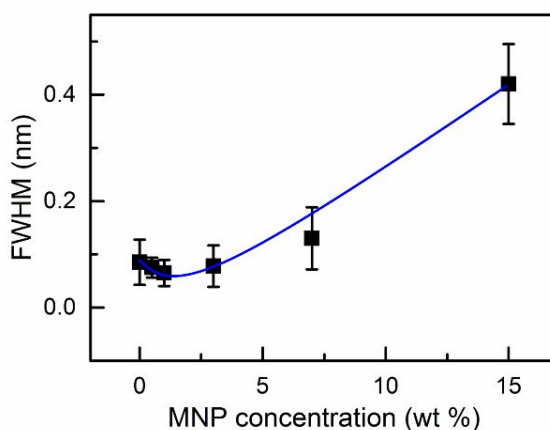


Figure S6. Values of full width at half maximum as a function of MNP concentration. Data are extracted from fitting the horizontal line cuts. The blue line presents a guide to the eyes.

References:

1. Rawolle, M.; Körstgens, V.; Ruderer, M.; Metwalli, E.; Guo, S.; Herzog, G.; Benecke, G.; Schwartzkopf, M.; Buffet, A.; Perlich, J.; Roth, S. V.; Müller-Buschbaum, P. Comparison of Grazing Incidence Small Angle X-Ray Scattering of a Titania Sponge Structure at the Beamlines BW4 (DORIS III) and P03 (PETRA III). *Rev. Sci. Instrum.* **2012**, 83, 106104.
2. Buffet, A.; Rothkirch, A.; Döhrmann, R.; Körstgens, V.; Abul Kashem, M. M.; Perlich, J.; Herzog, G.; Schwartzkopf, M.; Gehrke, R.; Müller-Buschbaum, P. P03, the Microfocus and Nanofocus X-Ray Scattering (MiNaXS) Beamline of the PETRA III Storage Ring: The Microfocus Endstation. *J. Synchrotron Radiat.* **2012**, 19, 647–653.